Development of low dark current SiGe-detector arrays for visible-NIR imaging sensor

Development of Low Dark Current SiGe-Detector Arrays for Visible-NIR Imaging Sensor

Ashok K. Sood, Robert A. Richwine and Yash R. Puri
Magnolia Optical Technologies Inc., 52-B Cummings Park, Woburn, MA 01801

Nicole DiLello, Judy L. Hoyt and Tayo I. Akinwande
Microsystems Technology Laboratories, MIT, Cambridge, MA 02139

Stuart Horn
DARPA/MTO, 3701, North Fairfax Drive, Arlington, VA 22203

Raymond S. Balcerak
Ray M. Balcerak, LLC, VA 22203

Gary Bulman and Rama Venkatasubramanian
RTI International, 3040 Cornwallis Road, Research Triangle Park, NC 27709

Arvind I. D'Souza
DRS Sensors and Targeting Systems, 10600 Valley View St., Cypress, CA 90630

Thomas G. Bramhall
DARPA Programs Office, US Army, AMSRD, Redstone Arsenal, AL 35898

ABSTRACT

SiGe based Focal Plane Arrays offer a low cost alternative for developing visible- NIR focal plane arrays that will cover the spectral band from 0.4 to 1.6 microns. The attractive features of SiGe based IRFPA's will take advantage of Silicon based technology, that promises small feature size, low dark current and compatibility with the low power silicon CMOS circuits for signal processing. This paper discusses performance comparison for the SiGe based VIS-NIR Sensor with performance characteristics of InGaAs, InSb, and HgCdTe based IRFPA's.

Various approaches including device designs are discussed for reducing the dark current in SiGe detector arrays; these include Superlattice, Quantum dot and Buried junction designs that have the potential of reducing the dark current by several orders of magnitude. The paper also discusses approaches to reduce the leakage current for small detector size and fabrication techniques. In addition several innovative approaches that have the potential of increasing the spectral response to 1.8 microns and beyond.

TECHNICAL DISCUSSION

There is significant interest in developing low cost IR Sensors for a variety of applications such as low cost thermal imagers and the ability to detect and defeat incoming threats. There are several other technologies such as InGaAs, InSb and HgCdTe, which cover different part of the IR Spectrum. HgCdTe IR focal plane arrays are being developed for 3-5 and 8-14 micron applications [1]. InSb is being used for 3-5 micron applications [2].

*E-mail: aksood@magnoliaoptical.com

Infrared Technology and Applications XXXV, edited by Bjørn F. Andresen, Gabor F. Fulop, Paul R. Norton
Proc. of SPIE Vol. 7298, 72983D · © 2009 SPIE · CCC code: 0277-786X/09/$18 · doi: 10.1117/12.820896

Similarly InGaAs offers an attractive approach for Visible-NIR sensors that can cover spectral band up to 1.8 microns [3]. SiGe offers a low cost alternative for developing Vis-NIR sensors that will not require any cooling and can operate from 0.4 to 1.6 micron [4, 5]. The attractive features of SiGe based IRFPA's will take advantage of Silicon based technology with much larger substrates with up to 10 inch, that can promise very small feature size and compatibility with the Silicon CMOS circuit for signal processing. Large area silicon substrates have the potential of bring the cost down substantially compared with InGaAs. In addition, we will discuss new approaches that can further increase the spectral response to 1.8 microns and beyond.

Performance Modeling for SiGe Vis-NIR Sensor

Spectrally, muzzle flashes approximate a blackbody spectrum of 800K to 1200K sources, with additional high radiance peaks that can occur at the emission lines for water and for various incendiary chemicals that comprise the propellant. Muzzle flashes consist of an intermediate flash and a brighter secondary flash (unless suppressed) as shown in figure 1.The secondary flash is shown in red and can be approximated as 1200-1400 K blackbody in the SWIR band. The primary flash in blue is approximated as an 800-1000K source. For the flash simulations (SNR plots), a conservative 1000K blackbody source is used.

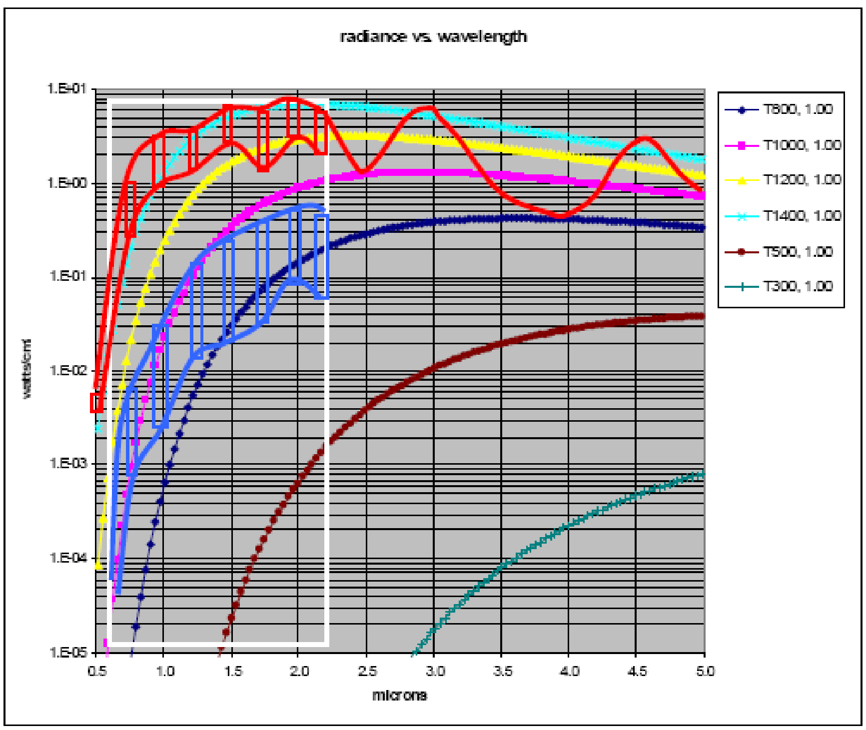

Figure 1: Plot of Flash Spectra as a function of wavelength from 0.5microns to 5 microns.

The dark current numbers used in the analysis were taken from measurements of Ge-on-Si photodiodes fabricated for high-speed on-chip integrated photonic applications [6]. These diodes were not optimized for imaging applications. The test diodes have sizes in the range of 10x10 to 200 x 200 microns. As the size of the detector is reduced below 10 microns further improvement in the detector dark current is expected, and will improve the sensor performance. These preliminary results show that with SiGe IR Sensor with f/2 optical system, one can detect targets of interest from over 1 km distance. This can have significant applications for a variety of defense missions. The detector sizes investigated here are for SiGe camera with (3, 5 and 7 microns) pixels. These simulations were performed to show the capability of megapixel SiGe Vis-NIR cameras.

As part of the simulations, detector dark currents were varied from 20 to 0.01 nano-Amps (nA). The spectral band used was 0.4-1.6 microns and the average quantum efficiency in band was 60%. An optical diameter of 2 inches, a focal length of 5 inches, and a 3 micron pixel provide a detector IFOV linear distance of 1.0" at 1 km and, assuming a 2000x2000 format array, an IFOV of 2.7 degrees or 155 feet at 1 km.

Figure 2 summarizes multiple model runs using these parameters. The source radiance simulated is an extended blackbody from 900 K to 1500K which approximates some of the targets of interest. The red plots are for the 3 micron pixel, the green for the 5 micron pixel and the blue for the 7 micron pixel. Muzzle flash (primary and secondary) can be approximated as extended blackbody sources in the 900-1500K.

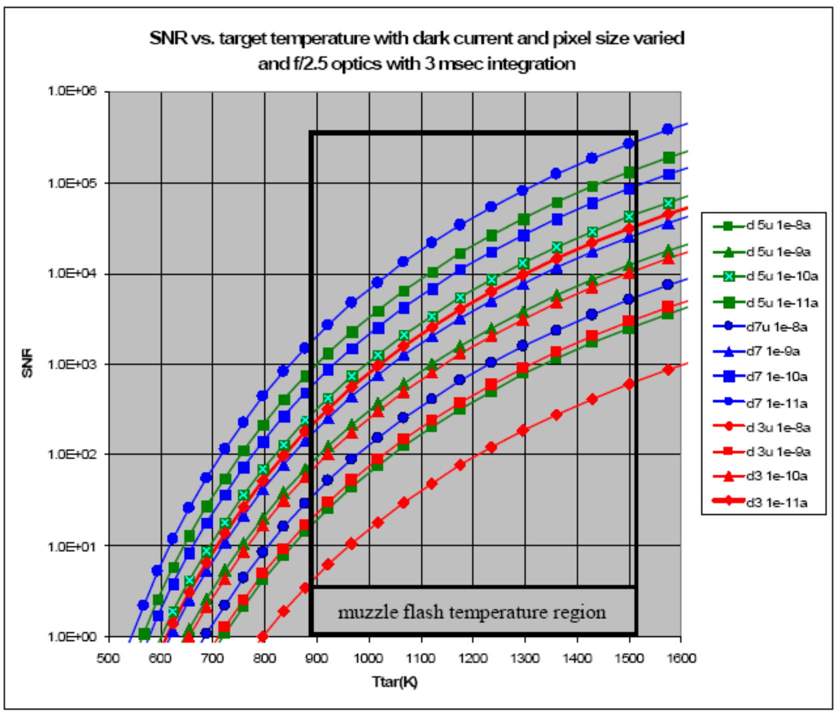

Figure 2: Signal to noise ratio (SNR) as a function of dark current for SiGe IRFPA for three unit cells size ranging from 3, 5 and 7 micron for temperature region of interest

Dark currents in SiGe detectors can be reduced by reducing the pixel size since dark currents track with the volume of the pixel. Reductions in size are advantageous for resolution; however, since the nightglow level is low, a large pixel size or at least a large collection area is required. If a high density (high fill factor) is achieved in these SiGe arrays, electronic pixel binning of small pixels can be used to achieve a reasonable sensitivity (NEI). If not, a microlens can be used to focus 20-25 micron collection area onto a smaller pixel. These two cases are investigated here using NEI (noise equivalent irradiance) and NEDR (noise equivalent differential reflectance) as performance metrics. NEI is in units of photons/sec-cm^2. NEDR is defined as the difference in target reflectance that provides a signal-to-noise of one under "standard" nightglow irradiance. In figure 3, the three plots are for a 20, 10 and 8.5 micron pixel SiGe detector.

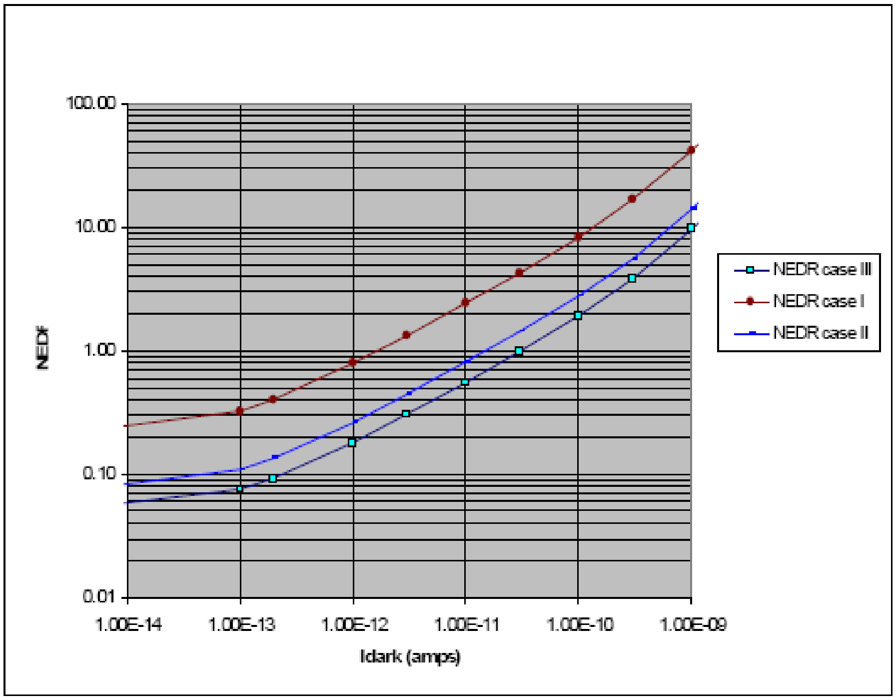

Figure 3: NEDR as a function of Dark Current for pixel size of 20, 10 and 8.5 microns for VIS-NIR spectral band (0.4 to 1.6)

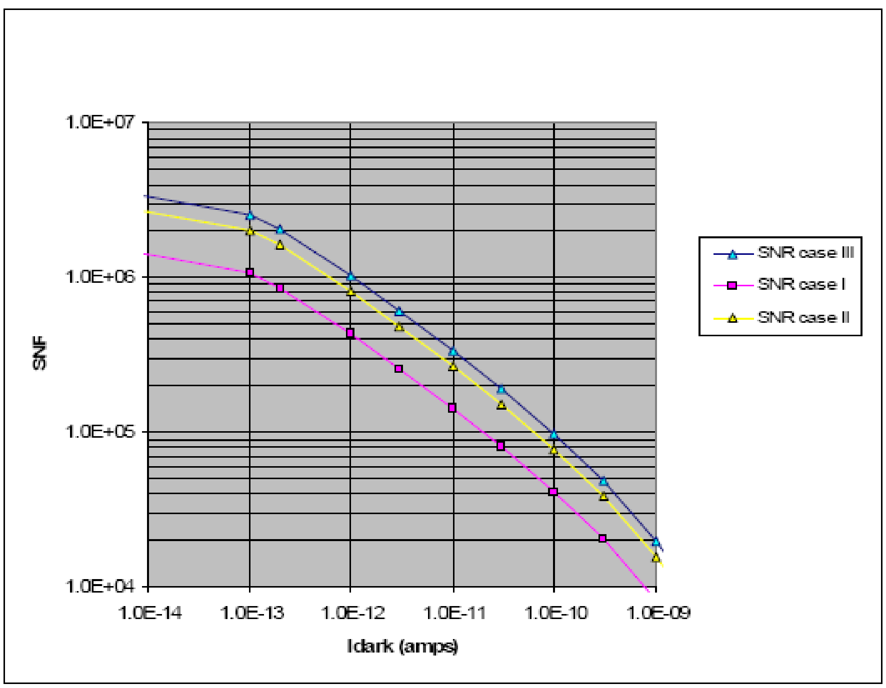

Figure 4: Signal to noise ratio (SNR) as a function of dark current for SiGe IRFPA

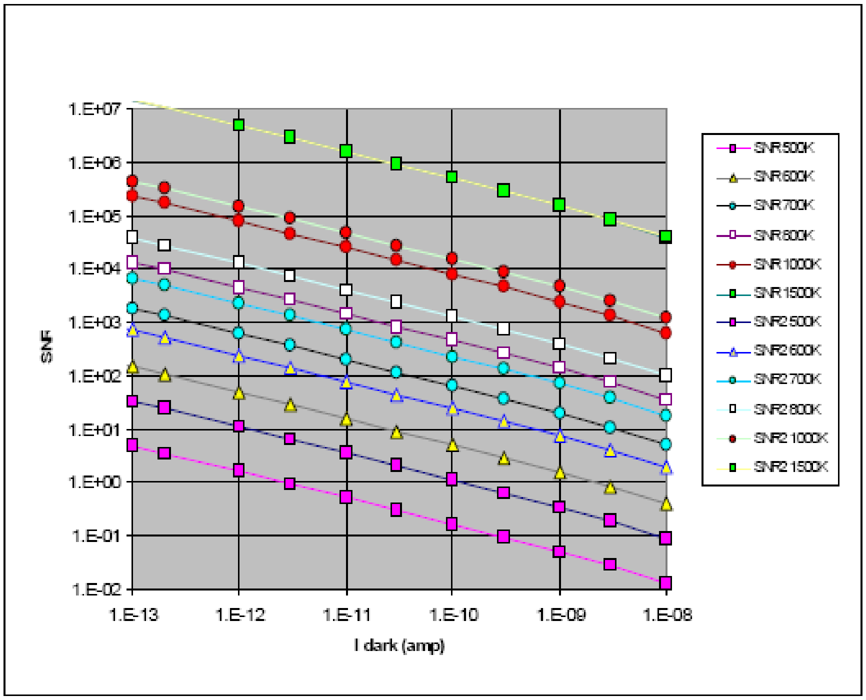

Figure 5: SNR vs. dark current for various target temperatures (radiances) for SiGe Vis-NIR Sensor

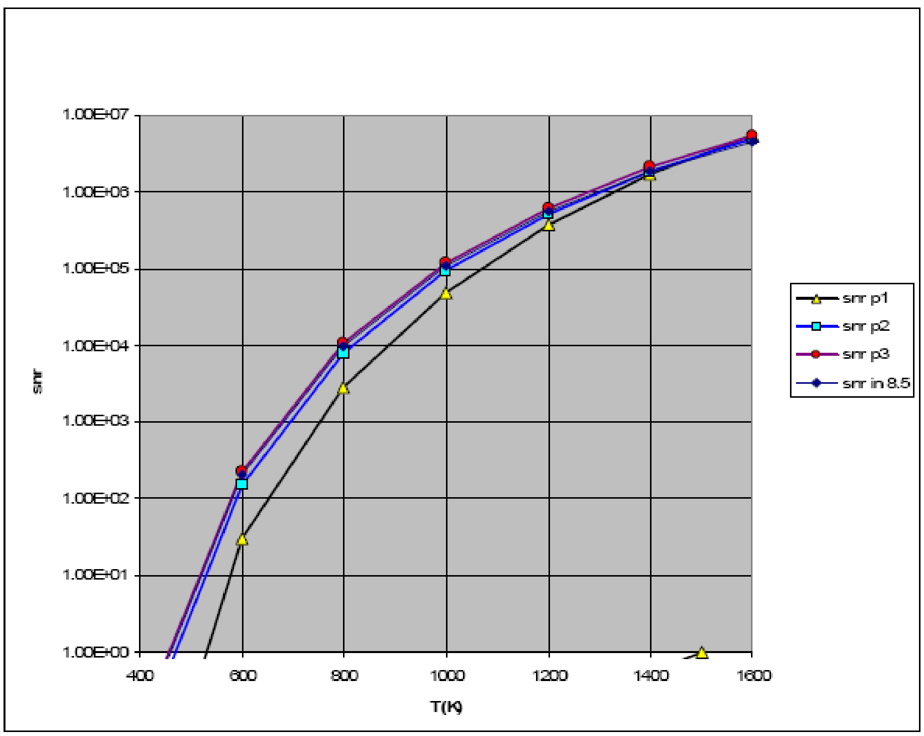

Figure 6: SNR vs. Target temperature for SiGe Vis-NIR Sensor

Figure 4 presents SNR's from a 1000K blackbody source for the SiGe FPA's with 20 microns, 10 microns and 8.5 microns respectively. The optics for all was at f/1, the integration time was 1 msec, and the number of read noise electrons from the ROIC was assumed to be 125. A simulation of SNR from various flash temperatures on sensor performance when detecting lower energy (temperature) events is shown in figures 5. Figure 6 presents Signal to Noise ratio (SNR) as a function of Target temperature for VIS-NIR Sensor. The analysis shows that a SiGe Sensor with room temperature operation has the ability to detect targets at 1Km and other plume detection at longer ranges. The results clearly demonstrate that SiGe sensor will have a variety of applications for Army missions.

Measured Characteristics of Ge-on-Si Photodiodes

To efficiently access the Vis-NIR band for various applications, high-Ge-content $Si_{1-x}Ge_x$ ($x > 0.5$) layers are required. Previous studies have demonstrated Ge-on-Si photodiodes with epitaxial material grown by ultra-high vacuum chemical vapor deposition [7] and by low-pressure chemical vapor deposition [6]. The Ge-on-Si diodes measured in this study were targeted for on-chip photonic applications, and details of the fabrication are described in [8].

Briefly, the devices are *pin* photodiodes fabricated in 1 μm-thick Ge layers grown selectively in oxide windows on 6" Si substrates, using low-pressure chemical vapor deposition in an Applied Materials epitaxial growth system [9]. Some of the wafers received an in-situ cyclic anneal between 830°C and 400°C to reduce the threading dislocation density while others were left unannealed. After Ge growth, the wafers were then implanted with phosphorus to create vertical *pin* junctions and contacted with metal. A schematic cross-section of these diodes is shown in the inset to Figure 7.

Figure 7 shows the measured current vs. voltage characteristics for 5 x 10 μm devices on both the annealed and the unannealed wafers. The cyclic anneal reduces the leakage current at -1 V by a factor of approximately 5, from 10 nA to 2 nA, on the lowest leakage diodes; however, the cyclic anneal also results in a larger distribution of the dark current.

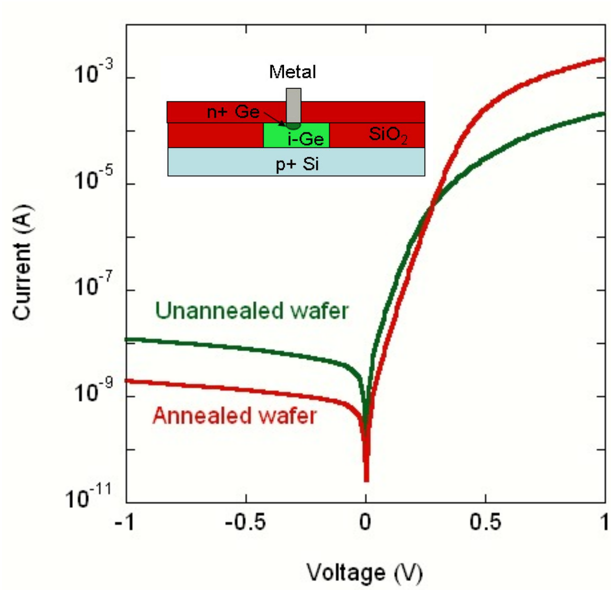

Figure 7: Current vs. voltage characteristics for 5 x 10 μm rectangular diodes. The cyclic anneal reduces the leakage current by ~5x for the best performing diodes. There is a large variation in dark current for devices on the annealed wafer. The inset shows a cross-sectional schematic of the device.

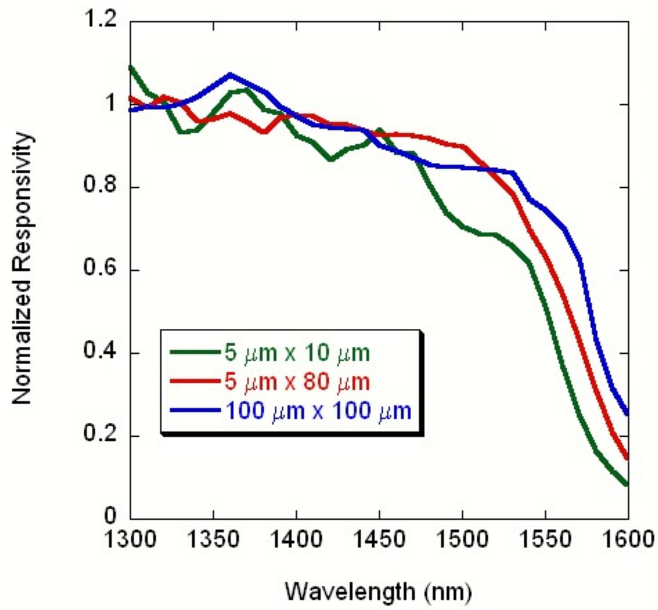

Figure 8: Normalized responsivity vs. wavelength for various sizes of rectangular diodes. The photoresponse was normalized to an average of values taken in the 1300–1350-nm range. The absorption edge shifts to longer wavelengths for larger devices, corresponding to a smaller bandgap. This smaller bandgap is consistent with larger strain in the larger area devices.

Figure 8 shows the normalized photoresponse for various sizes of diodes from the annealed wafer with an applied bias of -1 V. The absorption edge shifts to longer wavelengths for larger devices, suggesting a smaller bandgap (shrinkage of ~25 meV) in the larger Ge areas, resulting from the induced strain in the film [10]. This behavior in the responsivity is consistent with Raman analysis, which shows higher strain in the larger-area devices. At -1 V and 1550 nm, the 5 x 10 μm device has a responsivity of 0.18 A/W.

Further work is underway to determine the device design improvements for further lowering the dark current and increasing the photoresponse for these devices. In particular, process induced strain is being investigated to further shrink the band gap and push the absorption edge beyond 1550 nm.

Si-Ge SL Detector Development

We are also exploring the use of strained layer detector approaches to extend the response of Si_xGe_{1-x} alloys, while also avoiding dislocation formation, is to use strain. Coherently strained Si_xGe_{1-x}/Si superlattices, where the alloy layer is in compression, have smaller band gap energies and therefore longer detector cutoff wavelengths [11, 12, 13]. Figure 9a shows the calculated fundamental, lowest energy, indirect band gap of unstrained and coherently strained $Si_{1-x}Ge_x$ alloys grown on Si (100) substrates. It shows the addition of compressive strain significantly can reduce the cutoff wavelength to 1.6 microns at a Ge composition of x~0.4.

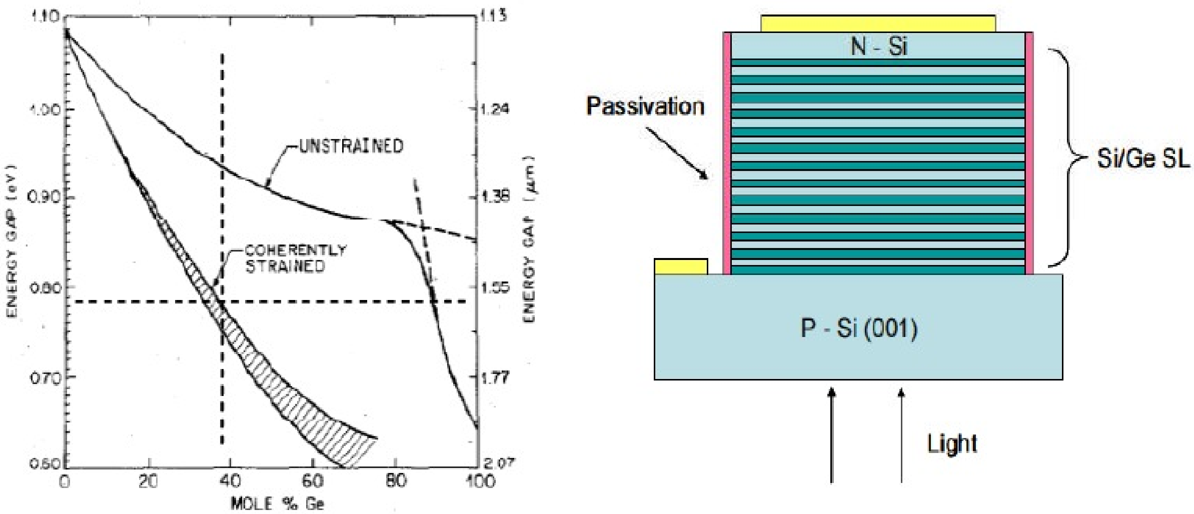

Figure 9: (a) Fundamental (lowest energy) indirect band gap of unstrained and coherently strained $Si_{1-x}Ge_x$ alloys grown on Si (100) substrates (from Ref. 12). (b) Proposed detector structure consisting of a $Si_{1-x}Ge_x$ /Si strained layer superlattice grown on (001) silicon.

Figure 9b shows the strained-layer superlattice (SLS) structure being pursued. It consists of $Si_{1-x}Ge_x$ quantum wells and Si barrier layers, grown on p-type (001) Si substrates. Superlattices having differing Si barrier and Ge well thicknesses to control the strain are grown to optimize wavelength response and dark current. The SiGe well thicknesses are kept below the critical layer thickness for dislocation formation. To complete the structure, the undoped superlattice is capped with a thin n^+ Si cap layer to form the p-n junction. After growth the devices are patterned with a top contact, mesas are etched to provide isolation and the substrate contact is formed. The etched mesa can also be passivated to minimize surface recombination as indicated in Figure 9b. The device shown in the figure uses substrate illumination, as is needed for use in FPA arrays, and short wavelength response can be improved by thinning the Si substrate. This device structure will be modified for VIS-NIR performance.

The strained-layer superlattices and quantum dot superlattices (QDSL) in the SiGe material system have the potential of developing Vis-NIR detector arrays with longer cutoff wavelength and potentially lower dark current. The advantage of quantum dots is the potential to exploit the optical properties of Ge while avoiding dislocation formation. Ge QDs grown on Si in Stranski-Krastanov mode can be deposited well beyond the critical thickness without dislocation nucleation. Figure 10a shows an SEM image of an array of Ge nanodots grown by MOCVD. These dots are typically 50-75 nm in diameter with area coverage of ~20%. A single layer of Ge QDs exhibits very low responsivity due to the finite absorption coefficient and is not desirable. To increase optical absorption and sensitivity, RTI has developed MOCVD-based growth techniques for the deposition of Ge/Si quantum dot superlattices (QDSLs), where Ge QDs are alternated with thin (10-30 nm) Si barrier layers. A cross-sectional TEM image of QDSLs is shown in Figure 10b.

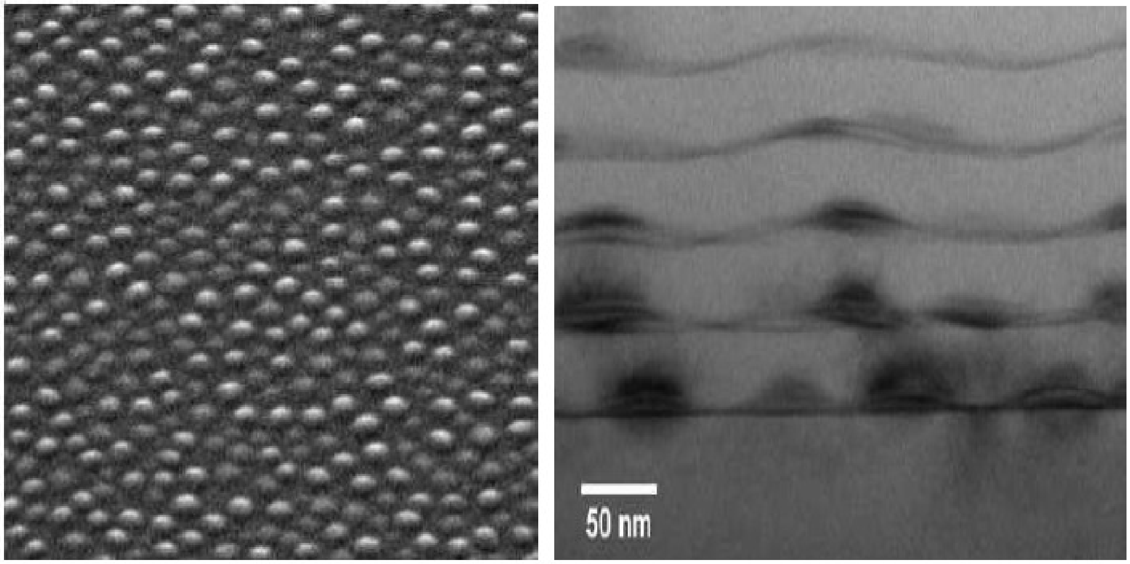

Figure 10: (a) SEM image (45° tilt) of a Ge QD layer deposited on Si. The QDs are ~60 nm in diameter with a density of 10^{20} cm^2. (b) Cross-sectional TEM image of Ge/Si QDSL grown. Ge QDs appear with dark contrast compared to Si barriers.

The use of Ge quantum dot superlattices or strained SiGe quantum wells is a very promising path towards achieving a Visible-SWIR imager on a Si platform. Low dislocation densities can be maintained in such structures, allowing dark current to be minimized, while sensitivity can be tuned by adding more periods to the superlattice. This approach allows the potential of achieving SiGe based detector arrays with cutoff wavelengths out to 2 microns. Significant effort is needed to explore the potential of these innovative structures for longer spectral response than 1.6 microns and very low dark currents in the order of 1 to 10 nAmp per cm^2.

As the technology for low dark current SiGe detector arrays is developed, further effort will be needed for fabricating high density large format SiGe Vis-NIR focal plane arrays[14]. The front side illuminated process has been developed by DRS for other IR sensor application such as HgCdTe, Si-MEMS based Microbolometers. The process flow shown in figure 11 provides various steps for the fabrication Process.

The fabrication and the integration process shown in figure 11 is shown with Silicon on Insulator (SOI) wafers. The SOI wafers have a thin, CMOS quality silicon layer on top, and a buried oxide layer. Detector p+ base layer and the intrinsic (i) layer are deposited by Si-Ge epitaxy (step1). Vias into Si-Ge are etched by RIE and the buried oxide layer provides the etch stop. Next we deposit an oxide layer to provide dielectric isolation for the via structure. Doped polysilicon deposition completes the top layer (n+) of the photodiode structure (p-i-n) and provides a conductive path to the opposite site of the detector (step 3). A silicon handle is bonded to the detector wafer (step 4) to provide support during the etching and thinning (step 5). The buried oxide layer provides an excellent stop (selectivity > 1000:1) when using EDP for silicon etch. Next, vias are opened though the oxide to access the top detector layer (n+) and the p+ base layer. This step is followed by via metal fill.

The detector wafer will be ready for bonding to CMOS. Direct bond interconnect brings to bear state of the art 3-D interconnect technology: wafer scale, low temperature process, highest density of electrical connections and ultra- small pitch, allowing the pixel scale reductions. Following bonding, the handle wafer is removed and pixel isolation etch completes the detector array (step 9).

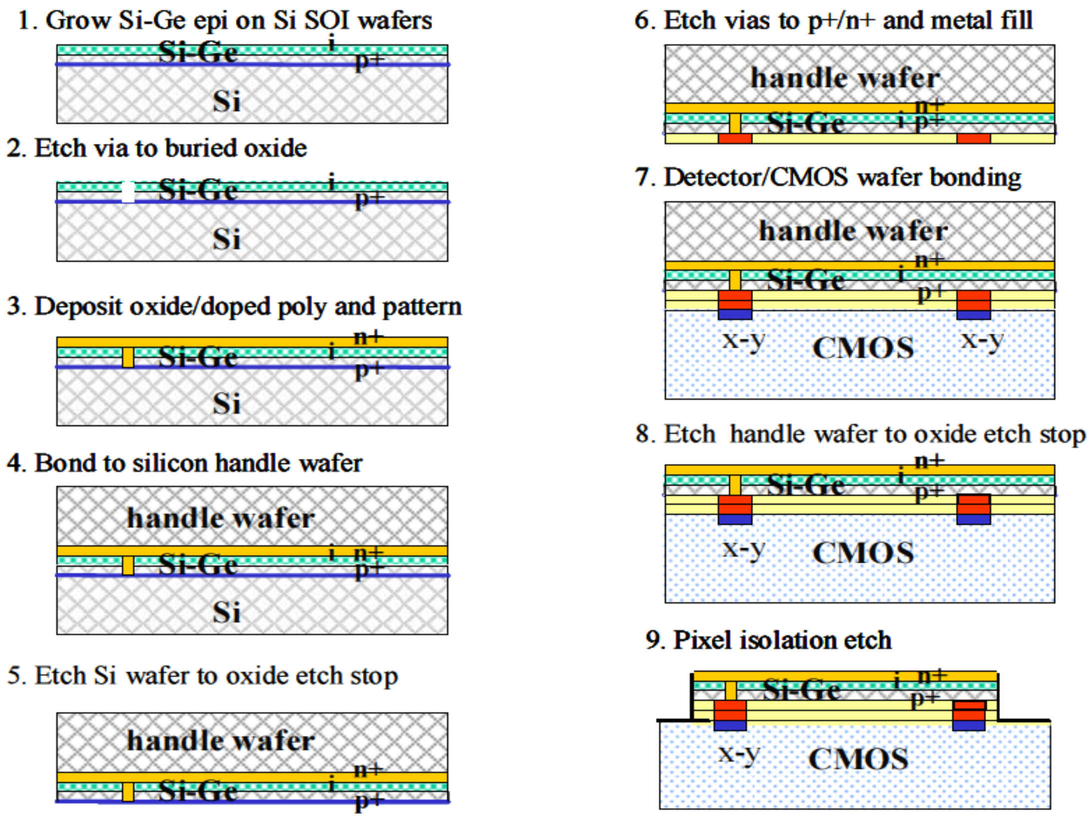

Figure 11: Process Flow for fabrication of VIS-NIR Front side illuminated SiGe FPA & CMOS ROIC for SiGe Sensor and Imager Applications

SUMMARY

SiGe based Vis-IR Focal Plane Arrays offer a low cost alternative for developing near IR sensors that will not require any cooling and can operate in the visible and NIR bands. The attractive features of SiGe based IRFPA's will take advantage of Silicon based technology, that promises small feature size and compatibility with the low power silicon CMOS circuits for signal processing.

A feasibility study of an infrared sensor based on Ge-on-Si photodiodes indicates promise for IR focal plane arrays with a spectral cutoff wavelength of 0.4 to 1.6 microns. Selective epitaxial growth, reduction of the diode size, and optimization of the diode structure to reduce tunneling leakage are expected to further reduce the dark current in these devices. We have also discussed potential application of SL and QD based structures that have the potential of extending the wavelength of operation beyond 1.8 micron to 2.0 micron. The challenge still remains to take advantage of these innovative device structures and further reduce the dark currents to 1 to 10 nAmp per cm^2.

ACKNOWLEDGEMENTS

The authors would like to thank Jung Yoon of MIT Lincoln Laboratory for device fabrication. The authors would also like to thank Jason Orcutt of MIT for access to his responsivity measurement station.

REFERENCES

1. H. Pollehn, K. K. Choi, S. Svensson and N. Dhar " IR Material Research at the Army research Labs" Proceedings of SPIE, Volume 6542, 65420C (2007)

2. J. O. Schlesinger et. al. " 640x512 InSb Detector Focal Plane Arrays" Proceedings of SPIE, Volume 6542, 6542031 (2007)

3. B. Onat, M. Ettenberg et. al. " Ultralow Dark current InGaAs Focal Plane Arrays" Proceedings of SPIE, Volume 6542, 654206 (2007)

4. F.Y Huang, et al. "Normal-incidence strained-layer superlattice SiGe/Si photodiodes near 1.3 um", Appl. Phys. Letters 67 (4), p. 566 (1995)

5. H. Temkin, et al, "GeSi strained-layer superlattice waveguide photo detectors operating near 1.3 um", Appl. Phys. Letters 45 (15), p. 963 (1986)

6. F. X. Kärtner, et al. "Electronic Photonic Integrated Circuits for High Speed, High Resolution, Analog to Digital Conversion," Proceedings of SPIE, 6125 (03), (2006).

7. J. Liu, et al., "Tensile strained Ge p-i-n photodetectors on Si platform for C and L band telecommunications," Appl. Phys. Letters **87** 011110 (2005).

8. M. Kim, O. Olubuyide, J. Yoon, and J.L. Hoyt, "Selective Epitaxial Growth of Ge-on-Si for Photodiode Applications," Electrochemical Society Transactions, 16 (10), pp. 837 – 847 (2008).

9. O. O. Olubuyide, et al., "Impact of Seed Layer on Material Quality of Epitaixal Germanium on Silicon Deposited by Low Pressure Chemical Vapor Deposition," Thin Solid Films, Vol. 508, p. 14 (2006)

10. Y. Ishikawa, K. Wada, D.D. Cannon, J. Liu, H-C. Luan, and L.C. Kimerling, "Strain-induced band gap shrinkage in Ge grown on Si substrate," Appl. Phys. Letters, 82 (13), pp. 2044 – 2046 (2003).

11. R. People "Physics and Applications of GeSi/Si Strained Layer Heterostructures" IEEE J. Quantum Electronics **QE-22** (1986), pp. 1696-1986.

12. M. L. Lee and R. Venkatasubramanian "Effect of nanodot areal density and period on thermal conductivity in SiGe/ Si nanodot superlattices" Appl. Phys. Lett. **92**, 0534112 (2008).

13. R.M. Kurtz, K.A. Alim, R.D. Pradhan, V. Esterkin, G. D. Savant, R. Venkatasubramanian, M.L. Lee, S. Ghosh, I. Calizo and A.A. Balandin " High Speed Nano-Optical Photodetector for Free Space Communications" Proc. SPIE **6556** (2007), 6556OH.

14. A.K. Sood, R.A. Richwine, Y. R. Puri, N. DiLello, J. L. Hoyt, T.I. Akinwande, R. S. Balcerak, S. Horn, T. G Bramhall, D. J. Radack, " Design Considerations for SiGe- based NIR Imaging Sensor" Proceedings of SPIE, Volume 6940, 69400M (2008).